Journal of Physics G: Nuclear and Particle Physics

Medium corrections to nucleon-nucleon interactions

To cite this article: P J Dortmans and K Amos 1991 *J. Phys. G: Nucl. Part. Phys.* **17** 901

View the article online for updates and enhancements.

You may also like

- Thermalization and prethermalization in isolated quantum systems: a theoretical overview
Takashi Mori, Tatsuhiko N Ikeda, Eriko Kaminishi et al.

- Equilibration and macroscopic quantum fluctuations in the Dicke model
Alexander Altland and Fritz Haake

- Single-shot work extraction in quantum thermodynamics revisited
Shang-Yung Wang

Recent citations

- Microscopic optical potentials derived from ab initio translationally invariant nonlocal one-body densities
Michael Gennari *et al*

- Cross sections and analyzing powers for (p,np) reactions of H2, Li6 , and C12 at 296 MeV
T. Wakasa *et al*

- Elastic differential cross sections for space radiation applications
Charles M. Werneth *et al*

This content was downloaded from IP address 134.75.87.181 on 24/01/2022 at 02:45

J. Phys. G: Nucl. Part. Phys. 17 (1991) 901–918. Printed in the UK

Medium corrections to nucleon–nucleon interactions

P J Dortmans and K Amos

School of Physics, University of Melbourne, Parkville, 3052 Victoria, Australia

Received 20 August 1990, in final form 21 January 1991

Abstract. The Bethe–Goldstone equations have been solved for both negative and positive energies to specify two-nucleon G matrices fully off the energy shell. Medium correction effects of Pauli blocking and of the auxiliary potential are included in infinite matter systems characterized by Fermi momenta in the range 0.5 fm^{-1} to 1.8 fm^{-1}. The Paris interaction is used as the starting potential in most calculations. Medium corrections are shown to be very significant over a large range of energies and densities. On-the-energy-shell values of G matrices vary markedly from those of free two-nucleon (NN) t matrices which have been solved by way of the Lippmann–Schwinger equation. Off the energy shell, however, the free and medium-corrected Kowalski–Noyes f ratios are quite similar suggesting that useful models of medium-corrected G matrices are appropriately scaled free NN t matrices. The choice of auxiliary potential form is also shown to play a decisive role in the negative energy regime, especially when the saturation of nuclear matter is considered.

1. Introduction

It has been many years since Brueckner and his collaborators established a particularly useful form of nuclear many-body theory based upon the two-nucleon (NN) interaction. Practical requirements, to this day, require use of infinite nuclear matter systems as working approximations to actual (finite) nuclear matter. But Bethe (1968) in the development of a Thomas–Fermi theory of large finite nuclei, established that the connection, the local density approximation, was a good approximation scheme for densities in excess of 17 % of the central density. Therein he also noted the importance of damping effects due to the 'auxiliary' (self-consistent) potentials in the propagators of the Brueckner theory. Since then numerous studies have been reported in the literature with reviews of the topic referencing most (Bethe 1968, 1971, Sprung 1972, Tabakin 1972, Kohler 1975, Srivastava and Sprung 1975, Jeukenne *et al* 1976).

A major quest in studies of the nuclear many-body problem has been to define the nuclear mean field within which each and every nucleon moves; the existence of which is inferred by the success of (phenomenological) shell and optical models for nuclear systems. But that quest can only be pursued with a chance of success if proper treatment is made of medium effects within the Brueckner theory. In a recent article (Yuan *et al* 1989), the mean free path of nucleons within infinite nuclear matter was studied using an extended Skyrme interaction and allowing for Pauli blocking effects. At 100 MeV and normal central densities ($k_{\mathrm{F}} = 1.4\,\mathrm{fm}^{-1}$) Pauli blocking effects nearly doubled the free-particle collision result. Even so the calculated mean free paths fell quite short of the 'empirical' value. That should be due in part to the neglect of

0954-3899/91/060901+18$03.50 © 1991 IOP Publishing Ltd

the auxiliary field in the calculations, as suggested by Cheon (1988) who used the effective-mass approximation to that field in his estimates of the nucleon mean free path.

The choice for the form which the auxiliary field takes is also very important. The so called 'standard' choice, where the auxiliary potential is taken to be zero above the Fermi surface, has been found to be inadequate in describing many nuclear matter results. The continuation of the auxiliary field above the Fermi surface ('continuous' choice) has been shown to better describe many nuclear matter properties, such as the binding energy per particle and the imaginary component of the optical potential (Mahaux 1979). In fact, with the 'continuous' choice, the auxiliary potential defined herein is a first-order approximation to the (real part of) the optical potential itself whence one may compare with the results of previous calculations (Brieva and Rook 1977, Jeukenne *et al* 1976). However, as the auxiliary potential is only a first-order approximant to the actual optical potential, such comparisons are not of great value, especially since higher-order corrections are known to be most significant (Baldo *et al* 1990).

But all nuclear medium calculations require evaluation of the Bethe–Goldstone G matrix off the energy shell (off-shell). For example, in the analyses of knock-out reactions, it was found (Redish *et al* 1970) that extraction of nuclear properties became tenuous if 'conventional' on-shell approximations were made. Likewise proper (NN) G-matrix calculations with allowance for those medium corrections are very important in defining nucleon–nucleon interaction potentials in nuclear matter. Indeed, from his studies, Muller (1980) concluded that these effects can vary predictions of nuclear matter absorption potential strengths by as much as a factor of five from that obtained using the associated free NN t matrix. Also the fully off-shell NN t matrix is required even when one uses the simple single-scattering approximation to multiple-scattering theory of elastic and inelastic events (Redish and Stricker-Bauer 1987a, b). In calculations with such a theory, frequently a pseudo t matrix is used. A pseudo t matrix is a convenient functional form for the NN G matrix with parameters chosen so that its on-shell values fit selected data, such as NN phaseshifts. But as demonstrated by Redish and Stricker-Bauer, for such a procedure the off-shell continuations are then completely ambiguous. Intriguingly however, 'realistic' interactions as well as those obtained by inversion of the NN phaseshifts (Amos *et al* 1988b, Kirst *et al* 1989) have very similar off-shell characteristics. The problem, therefore, lies with the specific medium correction effects defining the medium-modified G matrix and/or with the conventional $t\rho$ approximation for the optical potential. The latter is certainly a problem as stressed by the review of Sinha (1975) and significant differences between observables calculated using a full folding model and using the conventional $t\rho$ approximation have been reported recently (Arellano *et al* 1989, 1990). In any event, a primary requirement of microscopic theories of nuclei and their interactions is to know how two-nucleon G matrices are influenced by the presence of a nuclear medium.

2. Two-nucleon G matrices in nuclear matter

Consider a nucleon of momentum $\boldsymbol{p}_\mathrm{o}$ in collision with another of momentum $\boldsymbol{p}_\mathrm{b}$ and which is embedded in infinite nuclear matter. The Fermi sea is defined by a momentum

k_F. This collision involves a relative and a (two-nucleon) centre of mass momenta

$$\begin{aligned} \boldsymbol{k}_o &= \frac{(\boldsymbol{p}_o - \boldsymbol{p}_b)}{2} \\ \boldsymbol{K} &= \frac{(\boldsymbol{p}_o + \boldsymbol{p}_b)}{2} \end{aligned} \tag{2.1}$$

respectively.

Since the energies of the incoming and struck nucleons (ignoring medium effects) are

$$\begin{aligned} \epsilon_o &= \frac{\hbar^2 p_o^2}{2m} \\ \epsilon_b &= \frac{\hbar^2 p_b^2}{2m} \end{aligned} \tag{2.2}$$

the total energy of the two particles is also

$$E(\boldsymbol{k}_o, \boldsymbol{K}) = \frac{\hbar^2}{m}(k_o^2 + K^2). \tag{2.3}$$

After the interaction an equivalent set of momenta can be, and is, defined as $\boldsymbol{p}'_o$, $\boldsymbol{p}'_b$, $\boldsymbol{k}'_o$ and $\boldsymbol{K}'$ ($\equiv \boldsymbol{K}$).

The two-nucleon G matrix in nuclear matter is then the solution of the Bethe–Goldstone equation,

$$G(\boldsymbol{k}', \boldsymbol{k}; \boldsymbol{K}) = V(\boldsymbol{k}', \boldsymbol{k}) - \int V(\boldsymbol{k}', \boldsymbol{q}) \left(\frac{Q(\boldsymbol{q}, \boldsymbol{K}; k_F)}{[E(\boldsymbol{q}, \boldsymbol{K}) - E(\boldsymbol{k}_o, \boldsymbol{K})]} \right) G(\boldsymbol{q}, \boldsymbol{k}; \boldsymbol{K}) \, \mathrm{d}\boldsymbol{q} \tag{2.4}$$

wherein $V(\boldsymbol{k}', \boldsymbol{k})$ is the two-nucleon interaction in momentum space, $Q(\boldsymbol{q}, \boldsymbol{K}; k_F)$ is the Pauli blocking operator

$$Q(\boldsymbol{q}, \boldsymbol{K}; k_F) = \begin{cases} 1 & \text{if } |\boldsymbol{q} \pm \boldsymbol{K}| > k_F \\ 0 & \text{otherwise} \end{cases} \tag{2.5}$$

and the energy denominator (with medium effects included via the auxiliary potential $U(|\boldsymbol{k}_o + \boldsymbol{K}|)$) is now defined (Haftel and Tabakin 1970) by

$$\begin{aligned} [E(\boldsymbol{q}, \boldsymbol{K}) - E(\boldsymbol{k}_o, \boldsymbol{K})] = {} & \frac{\hbar^2}{m}(q^2 - k_o^2) \\ & + U(|\boldsymbol{q} + \boldsymbol{K}|) + U(|\boldsymbol{q} - \boldsymbol{K}|) - U(|\boldsymbol{k}_o + \boldsymbol{K}|) - U(|\boldsymbol{k}_o - \boldsymbol{K}|). \end{aligned} \tag{2.6}$$

Both the Pauli blocking and the energy denominator are functions of the integrating momentum angles and it is very convenient to approximate them by appropriate angle-averaged values. Thereby standard multipole expansions can be made to give the coupled set of integral equations defining the channel $\{(\alpha) \equiv JLL'ST\}$ G matrices, namely:

$$\begin{aligned} G_{LL'}^{(\alpha)}(k', k; K) = {} & V_{LL'}^{(\alpha)}(k', k) \\ & + \left(\frac{2}{\pi}\right) \sum_l \int_0^\infty V_{Ll}^{(\alpha)}(k', q) \left(\frac{\bar{Q}(q, K; k_F)}{[\bar{E}(q, K) - \bar{E}(k_o, K)]} \right) G_{lL'}^{(\alpha)}(q, k; K) q^2 \, \mathrm{d}q \end{aligned} \tag{2.7}$$

in which bars designate angle-averaged values. Specifically, the angle-averaged Pauli operator is

$$\bar{Q}(q, K; k_{\mathrm{F}}) = \begin{cases} 1 & \text{if } q \geq |K + k_{\mathrm{F}}| \\ 0 & \text{if } q < |K - k_{\mathrm{F}}| \\ \dfrac{(q^2 + K^2 - k_{\mathrm{F}}^2)}{2qK} & \text{otherwise.} \end{cases} \tag{2.8}$$

In the context of saturation of nuclear matter (negative 'incident' energies), Legindgaard (1978) has shown that this angle averaging is an accurate approximation, and Cheon and Redish (1989) have demonstrated that such accuracy remains when positive energies of 300 MeV and normal nuclear matter densities are considered. No such detailed calculation of the accuracy of angle averaging of the energy denominator exists but a convenient approximation is to use

$$\bar{E}(k, K) = \left(\frac{\hbar^2}{m}\right)(k^2 + K^2) + U(p_{\mathrm{o}}) + U(p_{\mathrm{b}}) \tag{2.9}$$

where $U(q)$ are auxiliary potentials for both the incoming and struck nucleons. The effective-mass approximation results in the individual single-particle energies being

$$\epsilon(p_i) = \left(\frac{\hbar^2}{2m^*}\right) p_i^2 + U_i \tag{2.10}$$

where U_i is a constant. Since the total energy is the sum of the incoming and struck nucleon energies, we get

$$\bar{E}(k, K) = \left(\frac{\hbar^2}{m^*}\right)(k^2 + K^2) + (U_{\mathrm{o}} + U_{\mathrm{b}}) \tag{2.11}$$

with $(U_{\mathrm{o}} + U_{\mathrm{b}})$ another constant and the effective mass is

$$m^* = m\left(\frac{1}{1+x}\right). \tag{2.12}$$

We seek a better result and one in which the interplay between the auxiliary potential and the two-nucleon G matrix is taken into account. To do so, we must consider the arguments of the potential in (2.6) with the Brueckner angle-averaged prescription (Brueckner and Gammel 1958),

$$|\boldsymbol{k} \pm \boldsymbol{K}|^2 \approx K^2 + k^2 \pm \frac{2}{\sqrt{3}} kK \bar{Q}^{3/2}(k, K; k_{\mathrm{F}}) \tag{2.13}$$

and use an average value for K when determining the single-particle potential, namely:

$$\begin{aligned} K \to K_{\mathrm{ave}} &\equiv K_{\mathrm{ave}}(k_{\mathrm{o}}; k_{\mathrm{F}}, p_{\mathrm{o}}) \\ &= \begin{cases} (k_{\mathrm{o}}^2 - p_{\mathrm{o}}^2)^{1/2} & \text{if } 2k_{\mathrm{o}} \leq |k_{\mathrm{F}} - p_{\mathrm{o}}| \\ \left\{(k_{\mathrm{o}}^2 + p_{\mathrm{o}}^2) - \frac{1}{4}\left[(2k_{\mathrm{o}} + p_{\mathrm{o}})^2 - k_{\mathrm{F}}^2\right]\right\}^{1/2} & \text{if } |k_{\mathrm{F}} - p_{\mathrm{o}}| \leq 2k_{\mathrm{o}} \leq |k_{\mathrm{F}} + p_{\mathrm{o}}|. \end{cases} \end{aligned} \tag{2.14}$$

The latter of these approximations is reasonable since the kernels are slowly varying functions of K in the relevant integration range (Haftel and Tabakin 1970). Then the interplay between $U(\mathrm{p})$ and the on-shell G matrices is given by a sum over each contributing two-body channel, namely:

$$U(p_o) = \left(\frac{8\hbar^2}{\pi m}\right) \sum_{JT} (2J+1)(2T+1) \times \int_0^{|k_F+p_o|/2} X(k_o)\,\mathrm{Re}\left\{G_{LL}^{(\alpha)}(k_o, k_o; K_{\mathrm{ave}})\right\} k_o^2\,\mathrm{d}k_o. \tag{2.15}$$

The integration weight $X(k_o)$ is 1 for k_o in the range 0 to $(\frac{1}{2}|k_F - p_o|)$ fm^{-1} and

$$X(k_o) = \frac{1}{2p_o k_o}\left[\tfrac{1}{4}(k_F^2 - p_o^2) - k_o(k_o - p_o)\right] \tag{2.16}$$

for $\frac{1}{2}|k_F - p_o| < k_o \le \frac{1}{2}|k_F + p_o|$. The momentum k_o is an 'on-shell' relative momentum value which with the chosen values of k_F and p_o specify K_{ave}, in (2.15), by the relationship (2.14). The two-nucleon 'centre-of-mass energy' at which we shall evaluate G matrices is then $\hbar^2 K_{\mathrm{ave}}^2/m$. For positive energies the energy denominator in the integral term on the right-hand side of (2.7) may contain a pole and so for ease of calculation (2.7) is not solved directly. Instead the principal value of the integral is taken (Haftel and Tabakin 1970, Amos *et al* 1988a)

$$R_{LL'}^{(\alpha)}(k', k; K_{\mathrm{ave}}) = V_{LL'}^{(\alpha)}(k', k) + \left(\frac{2}{\pi}\right) \sum_{l} \mathbf{P} \int_0^{\infty} V_{Ll}^{(\alpha)}(k', q) \times \frac{\bar{Q}(q, K_{\mathrm{ave}}; k_F)}{[\bar{E}(q, K_{\mathrm{ave}}) - \bar{E}(k_o, K_{\mathrm{ave}})]} R_{lL'}^{(\alpha)}(q, k; K_{\mathrm{ave}}) q^2\,\mathrm{d}q \tag{2.17}$$

defining the purely real 'reaction' matrices which relate to the G matrices by way of

$$G_{LL'}^{(\alpha)}(k', k; K_{\mathrm{ave}}) = R_{LL'}^{(\alpha)}(k', k; K_{\mathrm{ave}}) - \mathrm{i}B(k_o) \sum_{l} R_{Ll}^{(\alpha)}(k', k_o; K_{\mathrm{ave}}) G_{lL'}^{(\alpha)}(k_o, k; K_{\mathrm{ave}}) \tag{2.18}$$

wherein

$$B(k_o) = \frac{2k_o^2 \bar{Q}(k_o, K_{\mathrm{ave}}; k_F)}{\left[2k_o + (2m/\hbar) U'(q)|_{k_o}\right]} \tag{2.19}$$

involves

$$U'(q) \equiv \frac{\mathrm{d}}{\mathrm{d}q}\left\{U(|\boldsymbol{q} + \boldsymbol{K}_{\mathrm{ave}}|) + U(|\boldsymbol{q} - \boldsymbol{K}_{\mathrm{ave}}|)\right\}. \tag{2.20}$$

Since the centre-of-mass momentum (K) is itself dependent upon the energy of the incoming nucleon and the Fermi momentum, both the G and R matrices are functions of these.

As is usual (Haftel and Tabakin 1970), only the real parts of the on-shell G matrices are used in the summations to define the (real) auxiliary potentials that enter the iteration of the Bethe–Goldstone equation. The range of momentum for which (2.15) is used to define the auxiliary potentials has been a point of discussion. A standard choice has been to set $U(p_o)$ to zero if p_o is greater than k_F though this in itself is not truly self-consistent as outside the Fermi surface a zero set potential does not give convergent G matrices when iterated. It has also been argued that a continuous choice of the auxiliary potential is more realistic as it allows for appropriate cancellation of some important higher-order terms (Mahaux 1979). Also, with the continuous choice, the correct behaviour of the imaginary component of the optical model potential in the vincinity of the Fermi surface can be estimated (Hufner and Mahaux 1972, Mahaux 1979).

Solution of the Bethe–Goldstone equations may also be obtained at negative energies. In this case the G matrices are purely real and the infinite matter calculation leads to the binding energy per particle via

$$\left(\frac{\mathrm{BE}}{A}\right) = \frac{3}{5}\epsilon_F + \left(\frac{4\hbar^2}{\pi m}\right)\sum_{JT}(2J+1)(2T+1) \times \int_0^{k_F}\left(1 - \frac{3k_o}{2k_F} + \frac{k_o^2}{2k_F^2}\right) G_{LL}^{(\alpha)}(k_o, k_o; \bar{K}_{\mathrm{ave}})k_o^2\,\mathrm{d}k_o \tag{2.21}$$

wherein ϵ_F is the Fermi energy $(\hbar^2 k_F^2/2m)$, k_o again represents the on-shell relative momentum and the average centre-of-mass momentum is now redefined (Haftel and Tabakin 1970) as

$$\bar{K}_{\mathrm{ave}}^2 \equiv \bar{K}_{\mathrm{ave}}^2(k_F, k_o) = \frac{3}{5}(k_F - k_o)\left(k_F + \frac{k_o^2}{3(2k_F + k_o)}\right). \tag{2.22}$$

The choice of the starting (NN) interaction as well as the auxiliary potential form markedly affects predictions of the binding energy per particle as we shall show later.

The utility of the R matrices at positive energies is that they reflect the off-shell character of the complete G matrices and that character can be displayed for any channel (coupled or uncoupled) by Kowalski–Noyes f ratios (Kowalski 1965, Noyes 1965), namely:

$$f_{LL'}^{(\alpha)}(k, k_o; K_{\mathrm{ave}}) = \frac{R_{LL'}^{(\alpha)}(k, k_o; K_{\mathrm{ave}})}{R_{LL'}^{(\alpha)}(k_o, k_o; K_{\mathrm{ave}})} \tag{2.23}$$

with $K_{\mathrm{ave}}(k_o; k_F, p_o)$. Note that this ratio emphasizes off-shell behaviour by scaling against the on-shell value so that one must always bear in mind the actual size of the denominator when considering any significance of f ratios.

The results of our calculations are presented and discussed in the following sections of this paper. First the on-shell R matrices for various channels, Fermi momenta and at various energies with the Paris interaction (Lacombe *et al* 1980) are presented in tabular form and the effects of medium modification to the free NN scattering values are identified. Then the auxiliary potentials are discussed in section 4 and the Kowalski–Noyes f ratios of the medium-modified R matrices are presented and discussed in section 5. Finally, the solutions of the Bethe–Goldstone equations for negative energies were used to generate the binding energy per particle in infinite nuclear matter via the Brueckner–Hartree–Fock approximation for both the continuous and standard choice of auxiliary potentials. Those results are presented and discussed in section 6.

3. Medium modifications and the on-shell *R* matrices

The Bethe–Goldstone equations have been solved using Pauli blocking alone (+PB) and then with the inclusion of the auxiliary potential(+PB + U). This auxiliary potential is determined self-consistently by solving (2.15) iteratively and will be discussed in the following section. The results obtained using infinite matter densities of 0.008, 0.068, 0.185 and 0.394 nucleons per fm^3 (corresponding to k_F values of 0.5, 1.0, 1.4 and 1.8 fm^{-1} respectively) with the Paris interaction and for energies (centre of mass) of 25, 50, 100, 200 and 500 MeV are displayed in tables 1 to 6 for various two-nucleon channels. It can be seen from (2.1) that, unlike the case for the free two-nucleon t matrices, the relative momentum, k_o, is not directly proportional to the incoming momentum, p_o. In calculations of the auxiliary potential, this is not a problem as those potentials involve integration of the G matrices over all possible relative momenta. But to investigate on-shell effects to the medium-modified R matrices, we have selected an arbitrary choice, $k_o = p_o/2$, as it is found that there is but slight variation in the R matrices for all allowed relative momenta at a given energy. Results have also been obtained for all other $J \leq 2$ channels and with the Reid interaction (Reid 1968). The medium-modified results will be compared with the solutions of the Lippmann–Schwinger equations; the values of which are identified by the label 'free'.

Table 1. On-shell R-matrix elements for the $^1S_0$ state Paris interaction.

E (MeV)	k_F (fm^{-1})	0.5	1.0	1.4	1.8
25	free	−1.000	−1.000	−1.000	−1.000
	+PB	−1.010	−0.968	−0.921	−0.867
	+PB + U	−0.936	−0.871	−0.844	−0.758
50	free	−0.396	−0.396	−0.396	−0.396
	+PB	−0.404	−0.429	−0.454	−0.468
	+PB + U	−0.393	−0.402	−0.399	−0.354
100	free	−0.052	−0.052	−0.052	−0.052
	+PB	−0.052	−0.050	−0.053	−0.040
	+PB + U	−0.047	−0.038	−0.015	−0.045
200	free	0.169	0.169	0.169	0.169
	+PB	0.171	0.177	0.185	0.205
	+PB + U	0.174	0.192	0.231	0.298
500	free	0.606	0.606	0.606	0.606
	+PB	0.608	0.607	0.602	0.605
	+PB + U	0.612	0.638	0.680	0.785

The results for the uncoupled channels $^1S_0$, $^1P_1$ and $^3P_0$ are given in tables 1, 2 and 3 respectively. Of these the $^1S_0$ results display the largest effects of medium modifications although for the larger densities, medium corrections to the on-shell R-matrix elements for the other channels are not insignificant. As may be expected at the lowest density ($k_F = 0.5$ fm^{-1}) the nucleons are almost free and medium corrections to the free NN R-matrix values are very slight; a few per cent variation at most. As the density increases however, the importance of medium corrections also increases although there are different energy-dependent traits for the Pauli blocking and the auxiliary potential contributions. In the $^1S_0$ channel, at 50 MeV, the two effects are

Table 2. On-shell R-matrix elements for the $^1P_1$ state Paris interaction.

E (MeV)	k_F (fm^{-1})	0.5	1.0	1.4	1.8
25	free	0.249	0.249	0.249	0.249
	+PB	0.251	0.266	0.282	0.294
	+PB + U	0.257	0.273	0.288	0.301
50	free	0.256	0.256	0.256	0.256
	+PB	0.257	0.261	0.276	0.286
	+PB + U	0.260	0.273	0.289	0.303
100	free	0.257	0.257	0.257	0.257
	+PB	0.257	0.257	0.260	0.267
	+PB + U	0.258	0.266	0.279	0.297
200	free	0.257	0.257	0.257	0.257
	+PB	0.256	0.256	0.257	0.258
	+PB + U	0.257	0.263	0.278	0.297
500	free	0.331	0.331	0.331	0.331
	+PB	0.329	0.325	0.327	0.328
	+PB + U	0.330	0.335	0.352	0.386

Table 3. On-shell R-matrix elements for the $^3P_0$ state Paris interaction.

E (MeV)	k_F (fm^{-1})	0.5	1.0	1.4	1.8
25	free	−0.272	−0.272	−0.272	−0.272
	+PB	−0.271	−0.261	−0.255	−0.251
	+PB + U	−0.265	−0.253	−0.248	−0.241
50	free	−0.157	−0.157	−0.157	−0.157
	+PB	−0.159	−0.162	−0.160	−0.160
	+PB + U	−0.158	−0.156	−0.150	−0.142
100	free	−0.006	−0.006	−0.006	−0.006
	+PB	−0.006	−0.005	−0.002	0.005
	+PB + U	−0.005	0.000	0.013	0.033
200	free	0.137	0.137	0.137	0.137
	+PB	0.136	0.140	0.146	0.154
	+PB + U	0.138	0.148	0.170	0.200
500	free	0.376	0.376	0.376	0.376
	+PB	0.376	0.373	0.376	0.379
	+PB + U	0.377	0.386	0.410	0.457

essentially compensating while at 100 MeV the auxiliary potential has the major effect. Pauli blocking again is of significance at 200 MeV but is of practically no consequence at 500 MeV. Similar effects are observed with the $^1P_1$ and $^3P_0$ values.

The coupled channels ($^3S_1$, $^3D_1$ and $^3S_1$–$^3D_1$) results are given in tables 4, 5 and 6 respectively. At the lowest energy (25 MeV) and for all densities the medium correction effects upon the free $^3S_1$ on-shell R matrices are noticeable. However the changes wrought with increasing density are quite severe with both Pauli blocking and the auxiliary potential conspiring (at 25 MeV) to diminish the free values by factors of 2.5 to 3.5. In this ($^3S_1$) channel, the two medium modifications are again compensatory to

Table 4. On-shell R-matrix elements for the $^3S_1$ state Paris interaction.

E (MeV)	k_F (fm^{-1})	0.5	1.0	1.4	1.8
25	free	−2.466	−2.466	−2.466	−2.466
	+PB	−2.499	−2.070	−1.496	−1.091
	+PB + U	−2.054	−1.426	−1.088	−0.684
50	free	−0.825	−0.825	−0.825	−0.825
	+PB	−0.847	−0.933	−0.886	−0.777
	+PB + U	−0.821	−0.771	−0.618	−0.375
100	free	−0.225	−0.225	−0.225	−0.225
	+PB	−0.227	−0.237	−0.243	−0.225
	+PB + U	−0.224	−0.210	−0.144	−0.005
200	free	0.069	0.069	0.069	0.069
	+PB	0.068	0.075	0.089	0.113
	+PB + U	0.071	0.093	0.153	0.254
500	free	0.481	0.481	0.481	0.481
	+PB	0.487	0.486	0.504	0.525
	+PB + U	0.492	0.527	0.604	0.784

Table 5. On-shell R-matrix elements for the $^3D_1$ state Paris interaction.

E (MeV)	k_F (fm^{-1})	0.5	1.0	1.4	1.8
25	free	0.150	0.150	0.150	0.150
	+PB	0.147	0.119	0.108	0.111
	+PB + U	0.147	0.119	0.109	0.111
50	free	0.206	0.206	0.206	0.206
	+PB	0.206	0.194	0.164	0.132
	+PB + U	0.207	0.193	0.162	0.140
100	free	0.239	0.239	0.239	0.239
	+PB	0.239	0.234	0.219	0.184
	+PB + U	0.239	0.234	0.214	0.176
200	free	0.230	0.230	0.230	0.230
	+PB	0.229	0.227	0.220	0.205
	+PB + U	0.229	0.225	0.214	0.189
500	free	0.200	0.200	0.200	0.200
	+PB	0.201	0.199	0.198	0.195
	+PB + U	0.200	0.199	0.199	0.193

a degree at 50 MeV for normal densities, while at 100 MeV the Pauli blocking effect is relatively slight. At the higher energies both effects increase the $^3S_1$ on-shell R-matrix values substantially. In the $^3D_1$ channel, variation from the free results occurs only at higher densities and then it is mostly due to the Pauli blocking contribution. In the off-diagonal channel, and at 25 MeV, Pauli blocking is the most substantial medium correction effect while the auxiliary potential corrections are dominant for higher energies and at saturation densities. But there is some uncertainty with regard to the proper behaviour of the auxiliary potential at high momentum. Indeed, the high energy phenomenological optical model potentials suggest that the auxiliary potential

Table 6. On-shell R-matrix elements for the $^3S_1$–$^3D_1$ state Paris interaction.

E (MeV)	k_F (fm^{-1})	0.5	1.0	1.4	1.8
25	free	−0.092	−0.092	−0.092	−0.092
	+PB	−0.142	−0.315	−0.363	−0.367
	+PB + U	−0.172	−0.325	−0.363	−0.370
50	free	−0.047	−0.047	−0.047	−0.047
	+PB	−0.059	−0.136	−0.240	−0.317
	+PB + U	−0.073	−0.178	−0.268	−0.315
100	free	−0.041	−0.041	−0.041	−0.041
	+PB	−0.044	−0.063	−0.098	−0.154
	+PB + U	−0.048	−0.086	−0.144	−0.196
200	free	−0.059	−0.059	−0.059	−0.059
	+PB	−0.059	−0.064	−0.073	−0.087
	+PB + U	−0.061	−0.076	−0.103	−0.131
500	free	−0.155	−0.155	−0.155	−0.155
	+PB	−0.155	−0.156	−0.159	−0.161
	+PB + U	−0.160	−0.166	−0.182	−0.210

should tend to 10 MeV at saturation densities. Thus we repeated the calculations at $k_F = 1.4$ fm^{-1} with an auxiliary potential forced to tend smoothly with momenta to 10 MeV. The auxiliary potential effects upon the high-energy R matrices were then considerably reduced from those given in the tables. The other states calculated (but whose results have not been shown) have R matrices that are at most slightly affected.

4. The structure of the auxiliary potentials

The auxiliary potentials, as specified in (2.15), i.e. per the Brueckner–Hartree–Fock approximation, and for Fermi momenta of 0.5 fm^{-1} and 1.4 fm^{-1} are shown in figures 1 and 2 respectively. The method of solution is to obtain values for the auxiliary potential using (2.15), replacing these into the energy denominator in (2.7) iteratively until convergence is obtained. The Paris interaction is used as the starting interaction in both calculations and individual state contributions to each final result are shown. The contributions of F and G channels were also included in the total result, although their contributions were found to be quite small.

The low-density results shown in figure 1 are dominated by S-wave contributions in the low-momentum region and those channels contribute significantly (50%) to 2.5 fm^{-1} thereafter. The nett result in momentum space is an attractive well of 20 MeV depth at p_o of 0.3 fm^{-1}. Thus at low energies (S-wave) R matrices will be affected by this (low-density) auxiliary potential and such was observed in the on-shell values presented in table 1. Also, at low momenta, this auxiliary potential cannot be represented by an effective-mass approximation, namely $U \to -U_o + \alpha p_o^2$ as the potential actually decreases as $p_o \to 0$. In the vicinity of the Fermi momenta (0.5 fm^{-1}) however, the approximation is reasonable with parameter values (U_o, α) of (22.0, 1.7) that are equivalent to an effective-mass ratio (m^*/m) of 0.95.

With increasing Fermi momenta, the strength of the auxiliary potential increases and its shape changes to that of a central well with minimum (most negative) value

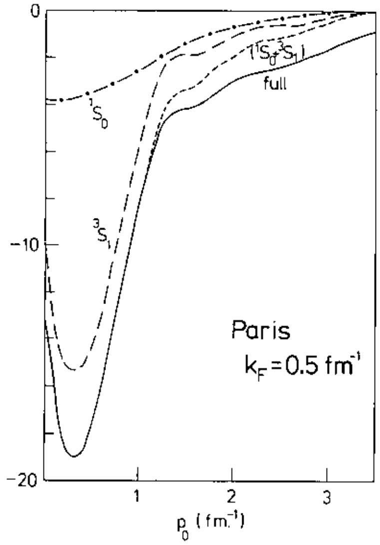

Figure 1. The auxiliary potential obtained using the Paris interaction as input to the Brueckner equations with a Fermi momentum of 0.5 fm^{-1} (approximately 5% of central nuclear saturation density). The component state contributions are as identified.

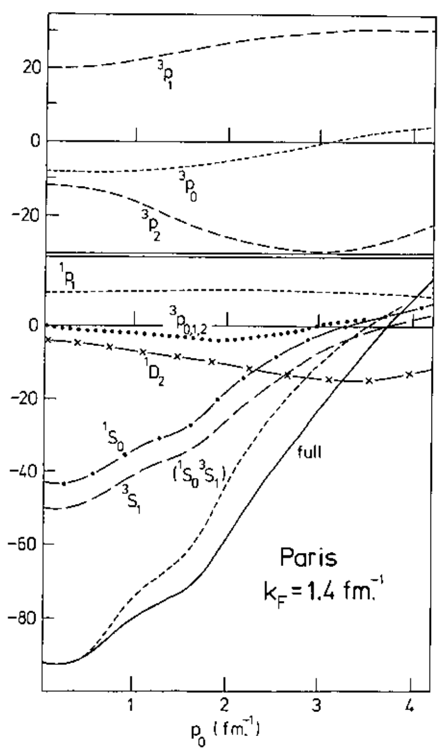

Figure 2. The auxiliary potential and its components obtained with the Paris interaction and a Fermi momentum of 1.4 fm^{-1}.

at zero momentum. The result starting with the Paris interaction and with a Fermi momentum of 1.4 fm^{-1} (essentially the central nuclear density value) is as shown by the full curve in figure 2. Component two-nucleon state contributions are identified in the figure with the summed ($^1S_0+^3S_1$) and ($^3P_{0,1,2}$) results given as well. In the upper portion of this figure the individual ^3P state contributions are displayed. The complete potential now has the form of a strong central attractive well with the S-channel contributions again dominant, and very much so in the range $0 < p_o < 0.5\ \mathrm{fm}^{-1}$. The higher partial waves contribute of the order of -10 MeV to this potential in the range $1 < p_o < 3\ \mathrm{fm}^{-1}$ but have the tendency to cancel. Clearly the $^1P_1$ and $^1D_2$ channel contributions are in opposition with an overall contribution which is insignificant, and the sum of the ^3P-channel potentials is much smaller than its constituent parts. The contribution due to other two-body channels is almost negligible. In the vicinity of the Fermi surface, an effective mass representation of this auxiliary potential is quite reasonable with parameter (U_o, α) values of (85, 5.36), i.e. with an effective-mass ratio of 0.88. We note that for small p_o the actual potential is of the order of 5 MeV deeper than the effective-mass estimate though this will only be important for nucleons with low incoming momenta. But in this region we may expect Pauli blocking to be the major nuclear medium effect. At higher momenta ($p_o > 5.0$ fm^{-1}), care must be taken with the two-body interaction potential being employed. In this region, the contribution of the higher two-body channels cannot be ignored. Even at the Fermi surface, channels other than the $^1S_0$ and $^3S_1$ contribute about 10% to the total auxiliary potential.

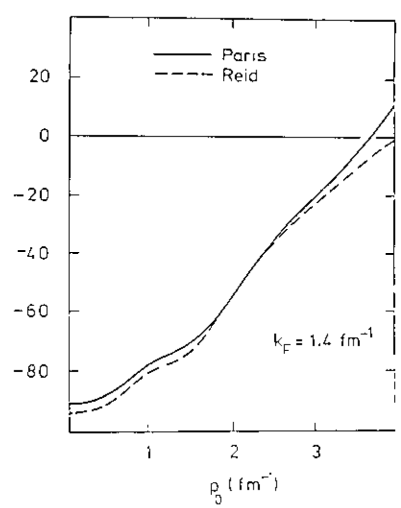

Figure 3. The auxiliary potentials obtained with a Fermi momentum of 1.4 fm^{-1} and using the Paris interaction (full curve) and the Reid interaction (broken curve).

As many two-body component contributions to the complete auxiliary potential cancel, the result is then quite sensitive to details. But such sensitivity is not serious in so far as using the auxiliary potential to generate R matrices within the nuclear medium since that potential enters only via the energy denominators. In any event, the auxiliary potentials for the Reid interaction are not very different *in toto* from those obtained using the Paris interaction as we display in figure 3. Therein the Reid

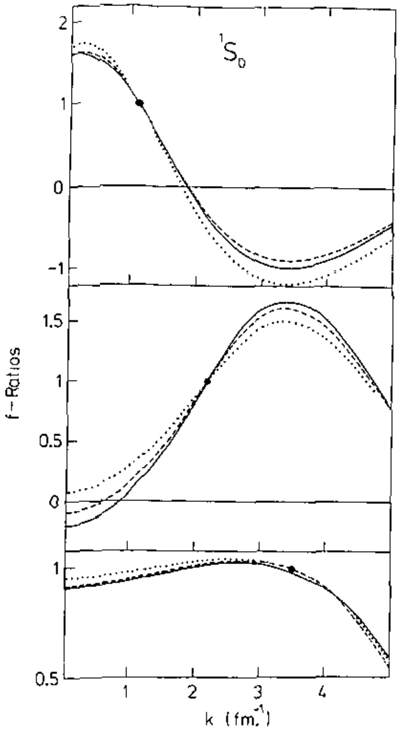

Figure 4. The Kowalski–Noyes f ratio (of R-matrix elements) obtained with a Fermi momentum of 1.4 fm^{-1} for the $^1S_0$ channel. The results obtained using (CM) energies of 50, 200 and 500 MeV are shown in the top, middle and bottom panels respectively. In each the free, Pauli blocked and Pauli blocked plus auxiliary potential calculations based upon the Paris interaction are shown by the full, broken and dotted curves respectively.

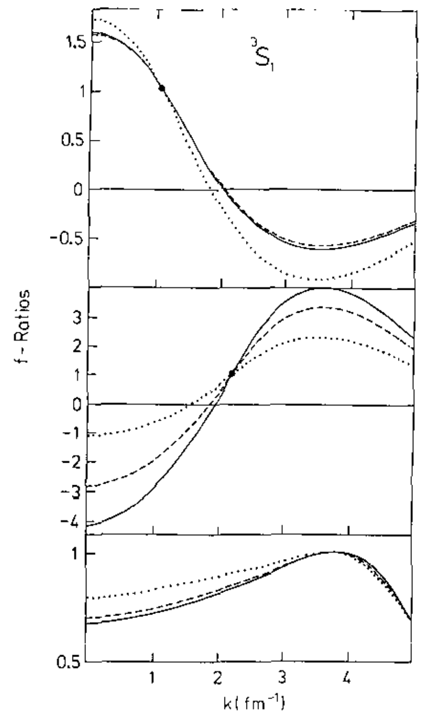

Figure 5. As for figure 4 but with the $^3S_1$ channel.

and Paris auxiliary potentials obtained at k_F of 1.4 fm^{-1} are compared. They differ substantially at higher values of momenta (> 4 fm^{-1}) but are quite similar otherwise. The problem of sensitivity is one that prevents simple identification of this auxiliary potential with the real part of the mass operator, and hence, optical potential.

5. Off-shell properties of R matrices

The off-shell properties of two-nucleon R matrices obtained with the Paris interaction are displayed by Kowalski–Noyes f ratios in figures 4, 5 and 6 for the $^1S_0$, $^3S_1$ and $^3P_1$ channels respectively. In each of the diagrams the f ratios at a Fermi momentum of 1.4 fm^{-1} are obtained using (CM) energies of 50, 200 and 500 MeV are presented in the top, middle and bottom panels respectively and for which the on-shell momenta are displayed by the dots. By definition, at those momentum values the f ratios are exactly one. In each, the free NN f ratio is depicted by the full curve and when Pauli blocking only is allowed then the results are those displayed by the broken curve. The complete results (Pauli blocking and auxiliary potentials) are shown by the dotted curves.

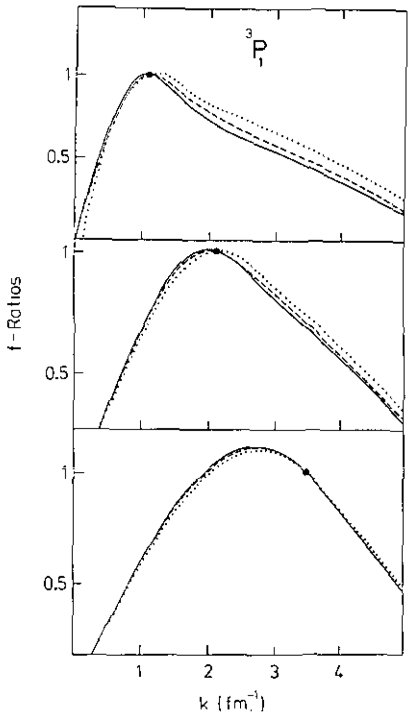

Figure 6. As for figure 4 but with the $^3P_1$ channel.

In all cases, the f ratios retain the trend of the free interaction off the energy shell. The variation of the S channels with energy reflects the change in sign of phaseshifts (on-shell t matrices) and medium modifications do not seriously alter the associated change in relative importance of R-matrix elements for momenta lower than to higher than the off-shell value. It is evident that Pauli blocking alone gives little change to off-shell behaviour of R matrices while inclusion of the auxiliary potential has more effect. But it seems unlikely that any calculation requiring these off-shell f ratios would display any difference from using the free NN values suitably scaled for the on-shell R-matrix value. The $^3S_1$ f ratios at 200 MeV (CM) are exceptional. But as with previous studies of free NN t matrices (Amos *et al* 1988a) in this region of energy we know that the on-shell R matrix is small and as this is the denominator of the f ratio, small (absolute) changes in values as one moves off the energy shell will reflect in large f ratio values.

Thus the primary effect of medium modifications is to vary the on-shell values of R matrices and a reasonable approximation for NN G matrices in nuclear matter may be to use those changed, on-shell strengths with the free NN t-matrix off-shell variations.

6. Binding energy per particle in infinite matter

As has been noted previously, there are two conventional choices made for the form of the auxiliary potentials above the Fermi surface. In most studies to date, the continuous choice of the auxiliary potential has been used preferentially with the justification that this choice more accurately describes actual properties of nuclear matter, specifically the binding energy per particle and saturation of nuclear matter. The effect of these alternate forms upon the binding energy per particle (2.21) is evident in figure 7. Clearly whether the Reid or Paris G matrices are used, the continuous choice gives much more binding at all Fermi momenta than does the standard choice of auxiliary potential. All results saturate albeit at too high a density and with too low a binding value. Mahaux (1979) assessed that using the standard choice in such calculations requires explicit evaluation of higher-order diagrams. In contrast, with the continuous choice, some of those higher-order diagrams almost cancel to give the final result of saturation at k_F of 1.45 fm^{-1} and with a binding of -15 MeV. It is known that contributions from higher-order diagrams (Grange 1979) and from Δ-isobar effects (Dey *et al* 1987) then change these results to give better agreement with the 'data'.

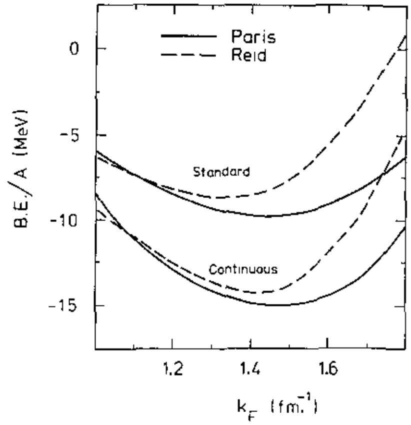

Figure 7. The binding energy per particle obtained from the Reid and Paris G matrices for different choices of the form of the auxiliary potential above the Fermi sea.

It is instructive to consider the contributions made channel by channel to the binding energy per particle as the Fermi momenta increases. Those contributions for k_F of 0.5, 1.0, 1.4 and 1.8 fm^{-1} are given in table 7. At the lowest density (k_F = 0.5 fm^{-1}) the S states give the dominant contributions: -6.03 and -4.45 MeV for the continous (C) and standard (S) auxiliary potential calculations respectively. The aggregate potential energy of all other channels is $+0.08$ and $+0.11$ MeV in those cases respectively. At higher densities contributions other than from the S channels are not negligible. At 1.0 fm^{-1} the P states essentially have magnitude in excess of 1 MeV whilst when k_F is 1.8 fm^{-1}, with rare exception, all channels contribute significantly. But whether the continous or standard choice is made, by and large the contributions from non-S-wave channels tend to cancel. In fact the sum of potentials from other than S states contributes 0.12 (0.33), -1.37 (-0.23) and -2.71 (-1.17) MeV in the continuous (standard) choice calculations with k_F values of 1.0, 1.4 and 1.8

Table 7. Contributions to the binding energy per particle by NN channels for a set of Fermi momenta. The results with G matrices obtained using the continuous choice for the auxiliary potential are given in columns headed C while those with the standard choice are listed under S.

k_F =	0.5		1.0		1.4		1.8	
State	C	S	C	S	C	S	C	S
$^1S_0$	−1.85	−1.61	−8.51	−8.25	−16.69	−16.34	−24.03	−23.85
$^3S_1$	−4.18	−2.84	−12.49	−10.60	−21.14	−17.50	−23.93	−21.42
$^3P_2$	−0.09	−0.08	−2.09	−2.00	−8.36	−8.00	−21.18	−20.80
$^3P_1$	0.21	0.21	3.32	3.39	11.35	11.74	28.62	29.25
$^3P_0$	−0.11	−0.11	−1.45	−1.44	−3.88	−3.82	−6.39	−6.32
$^1P_1$	0.10	0.11	1.51	1.53	4.78	4.89	11.05	11.19
$^3D_3$	0.00	0.00	0.06	0.02	0.03	0.12	0.22	0.37
$^3D_2$	−0.03	−0.02	−1.12	−1.10	−4.74	−4.65	−12.40	−12.30
$^3D_1$	0.01	0.01	0.38	0.39	1.67	1.68	4.38	4.40
$^1D_2$	−0.02	−0.02	−0.71	−0.71	−3.18	−3.16	−9.03	−8.99
$^3F_3$	0.01	0.01	0.36	0.36	1.84	1.84	5.41	5.41
$^3F_2$	−0.00	−0.00	−0.12	−0.12	−0.69	−0.69	−2.10	−2.10
$^1F_3$	0.00	0.00	0.20	0.20	0.97	0.97	2.75	2.75
$^3G_4$	−0.00	−0.00	−0.13	−0.13	−0.88	−0.87	−3.08	−3.07
$^3G_3$	0.00	0.00	0.03	0.03	0.25	0.25	0.93	0.93
$^1G_4$	−0.00	−0.00	−0.09	−0.09	−0.55	−0.55	−1.88	−1.88
KE	3.11	3.11	12.44	12.44	24.38	24.38	40.31	40.31
BE/A	−2.84	−1.23	−8.46	−6.08	−14.82	−9.69	−10.36	−6.13

fm^{-1} respectively. Thus it is the S states that eventually determine the binding energy per particle and the choice of standard or continuous form of auxiliary potentials in calculations has a quite marked effect therein. The results obtained using the Reid interaction are very similar to those listed for the Paris interaction in table 7 other than for the $^3S_1$ state at the highest densities.

7. Conclusion

On-shell, medium correction effects due to Pauli blocking and the auxiliary potential can be substantial. For normal nuclear matter densities and for all important two-body channels ($J \leq 2$), the on-shell values of the G matrices differ noticeably from those of the associated free t matrices. The two medium correction effects are found to vary markedly with both energy and density. At (CM) energies in the 50 to 100 MeV range they tend to interfere destructively in such a way that in some cases the on-shell G matrices, with both Pauli blocking and the auxiliary potential, and the free t matrices are very similar on-shell. At higher energies, the effect of Pauli blocking is reversed, so that now both the auxiliary field and the Pauli blocking contribute constructively. The Pauli exclusion corrections are most important for low energies and large densities while corrections due to the auxiliary potential are most significant for calculations made at the higher energies and, again, large densities. Their effects are most severe in the NN S channels and so these channels then dominate the prescription of the auxiliary potential itself (especially at low incoming nucleon momentum). This latter effect, however, is emphasized by the fact that the higher angular momenta states tend to give offsetting contributions to the potentials.

The off-shell properties of two-nucleon G matrices also differ from those of the free NN t matrices but their momenta variations as displayed by the Kowalski–Noyes f ratios are very similar. Indeed so similar that it suggests a useful 'model' for the extension of G matrices off-shell would be to use free, fully off-shell NN t matrices, scaled to give the pertinent, medium-corrected on-shell values.

Finally when calculating the binding energy per particle, it is seen that higher-order terms (even up to $J = 4$ states) give a significant contribution to the potential energy. Hence these channels cannot be ignored if one wishes to accurately obtain the binding energy per particle and the nuclear saturation. The choice of using a continuous potential as opposed to the standard prescription is also shown to be important, increasing the binding energy per particle by as much as 5 MeV near the saturation densities, and thus causing the calculated value to be closer to the known empirical result.

Acknowledgments

We are very grateful to Dr L Rikus of the Bureau of Meteorology Research Centre for providing the basic computer programs which, after suitable modifications gave a number of the results reported herein. We also acknowledge the fruitful discussions with Dr L Berge of the School of Physics, University of Melbourne and Professor H V von Geramb, Institut für Theoretische Physik, Universität Hamburg, Germany.

References

Arellano H F, Brieva F A and Love W G 1989 *Phys. Rev. Lett.* **63** 605
—— 1990 *Phys. Rev.* C **41** 2188
Amos K, Berge L, Brieva F A, Katsogiannis, Petris L and Rikus L 1988a *Phys. Rev.* C **37** 934
Amos K, Berge L, von Geramb H V and Coz M 1988b *Nucl. Phys.* A **499** 45
Baldo M, Bombaci I, Giansiracusa G, Lombardo U, Mahaux C and Sartor R 1990 *Phys. Rev.* C **41** 1748
Bethe H 1968 *Phys. Rev.* **167** 879
—— 1971 *Ann. Rev. Nucl. Sci* **21** 93
Brieva F A and Rook J R 1977 *Nucl. Phys.* A **291** 299
Brueckner K A and Gammell J L 1958 *Phys. Rev.* **109** 1023
Cheon T 1988 *Phys. Rev.* C **38** 1516
Cheon T and Redish E F 1989 *Phys. Rev.* C **39** 331
Dey J, Matin M A and Mahaux C 1987 *Z. Phys.* A **327** 33
Grange P 1979 *Nucl. Phys.* A **328** 104
Haftel M I and Tabakin F 1970 *Nucl. Phys.* A **158** 1
Hufner J and Mahaux C 1972 *Ann Phys., NY* **73** 525
Jeukenne J L, Lejeune A L and Mahaux C 1976 *Phys. Rep.* **25C** 83
Kirst Th, Amos K, Berge L,Coz M and von Geramb H V 1989 *Phys. Rev.* C **40** 919
Kohler H S 1975 *Phys. Rep.* **18** C 217
Kowalski K L 1965 *Phys. Rev. Lett.* **15** 798
Lacombe M, Loiseau B, Richard J M, Vinh-Mau R, Cote J, Pires P and de Tourreil R 1980 *Phys. Rev.* C **21** 861
Legindgaard W 1978 *Nucl. Phys.* A **297** 429
Mahaux C 1979 *Nucl. Phys.* A **328** 24
Muller K-H 1980 *Z. Phys.* A **295** 79
Noyes H P 1965 *Phys. Rev. Lett.* **15** 538
Redish E F, Stephenson Jr G J and Lerner G M 1970 *Phys. Rev.* C **2** 1665
Redish E F and Stricker-Bauer K 1987a *Phys. Rev.* C **35** 1183

—— 1987b *Phys. Rev.* C **36** 513
Reid R V 1968 *Ann. Phys., NY* **50** 411
Sinha B 1975 *Phys. Rep.* **20C** 1
Sprung D W L 1972 *Advances in Nuclear Physics* vol 5, ed M Baranger and E Vogt (New York: Plenum) p 225
Srivastava M K and Sprung D W L 1975 *Advances in Nuclear Physics* vol 8, ed M Baranger and E Vogt (New York: Plenum) p 121
Tabakin F 1972 *The Two-body Force in Nuclei* ed S M Austin and G M Crawley (New York: Plenum) p 119
Yuan H J, Lin H L, Fai G and Moszkowski S A 1989 *Phys. Rev.* C **40** 1448